ACS Catalysis

Research Article

pubs.acs.org/acscatalysis

Ambient Temperature Hydrocarbon Selective Catalytic Reduction of NO_x Using Atmospheric Pressure Nonthermal Plasma Activation of a Ag/Al_2O_3 Catalyst

Cristina E. Stere,[†] Wameedh Adress,[‡] Robbie Burch,[†] Sarayute Chansai,[†] Alexandre Goguet,[†] William G. Graham,*[,‡] Fabio De Rosa,[†,§] Vincenzo Palma,[§] and Christopher Hardacre*[,†]

[†]Centre for the Theory and Application of Catalysis, CenTACat, School of Chemistry and Chemical Engineering and [‡]Centre for Plasma Physics, School of Mathematics and Physics, Queen's University Belfast, University Rd, Belfast BT7 1NN, N. Ireland, U.K.

[§]Dipartimento di Ingegneria Industriale, Università di Salerno, Via Ponte Don Melillo 84084 Fisciano, SA, Italy

Supporting Information

ABSTRACT: Atmospheric pressure nonthermal-plasma-activated catalysis for the removal of NO_x using hydrocarbon selective catalytic reduction has been studied utilizing toluene and *n*-octane as the hydrocarbon reductant. When the plasma was combined with a Ag/Al_2O_3 catalyst, a strong enhancement in activity was observed when compared with conventional thermal activation with high conversions of both NO_x and hydrocarbons obtained at temperature ≤250 °C, where the silver catalyst is normally inactive. Importantly, even in the absence of an external heat source, significant activity was obtained. This low temperature activity provides the basis for applying nonthermal plasmas to activate emission control catalysts during cold start conditions, which remains an important issue for mobile and stationary applications.

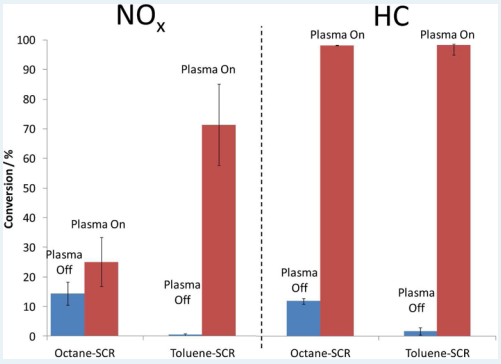

KEYWORDS: *Ag/Al_2O_3, nonthermal plasma, NO_x reduction, low temperature hydrocarbon selective catalytic reduction, toluene, n-octane*

1. INTRODUCTION

Catalysis is an essential enabling technology which impacts the quality and economics of our lives. It holds the key to solving many problems facing society, among which are automotive emission control and clean energy production. Stringent emission regulations have led to innovative research and the development of efficient technologies for pollution control both for stationary and mobile applications. Among these, selective catalytic reduction (SCR) by hydrocarbons (HC) has shown a high potential in the removal of NO_x emissions from diesel and lean-burn gasoline engines.[1−13] Ag/Al_2O_3 catalysts have been widely studied for this reaction as they have been shown to be highly selective to N_2 versus N_2O and have moderate tolerance to water vapor and SO_2.[5,8,9,12,13] However, a significant drawback of the Ag-based systems is their lack of activity below 350 °C; therefore, control of the reaction conditions would be key for practical use. These systems have significant issues associated with cold start conditions where very poor NO_x reduction activity is observed.

Recently, electrically produced plasma-based processes have been reported as an attractive alternative to conventional thermally activated reactions. This interest stems from the fact that often the highly reactive species in the plasma are not in thermodynamic equilibrium. Depending on the amount of energy and the details of how it is coupled into the plasma, the plasma can be classified as thermal or nonthermal. Nonthermal plasmas (NTPs) are in highly nonequilibrium state characterized by high temperature electrons of several thousands of degrees, although the background gas molecules/ions are close to ambient temperature. The main advantage of NTPs is that they can enable thermodynamically unfavorable reactions to occur at low temperatures; however, the selectivity toward the products of interest is not always optimal.[14,15] Therefore, the combination of heterogeneous catalysis with plasmas has attracted interest due to the combined possible advantages of having a fast and low-temperature reaction from atmospheric nonthermal plasma and high product selectivity from heterogeneous catalysis. Hybrid plasma−catalyst systems have proven to be very efficient in promoting the activity in VOC oxidation, automotive catalysis, water purification, and reforming/hydrogenation reactions.[15−24]

In many cases, the NTP is placed upstream of the catalyst bed[17,25,26] and activates the gas prior to contacting with the surface of the catalyst. For example, Rappé et al.[26] reported ∼80% reduction of NO_x in a simulated lean exhaust over a Ba/zeolite Y and Ag/ γ-alumina catalytic system at 200 °C with the

Received: October 16, 2013
Revised: December 18, 2013
Published: January 10, 2014

plasma upstream of the catalyst bed. Li et al.[9] also reported an increase in NO_x conversion from ~30% to >85% at 340 °C over silver-based catalysts when the reaction gas was activated by NTP. Cho and co-workers[27] studied the plasma-assisted hydrocarbon selective catalytic reduction (HC-SCR) system using oxygenated hydrocarbons produced by a diesel fuel reformer and reported the beneficial effect of a plasma on both the NO_x and HC conversion at 200 °C. Importantly, further enhancements were achieved by placing the catalyst in the discharge area.[9,18,28] Li et al.[9] studied the effect of plasma on the NO_x storage capacity (NSC) of a $Pt/Ba/Al_2O_3$ catalyst between 100 and 300 °C. Compared with only thermally activating the catalyst, an increase of up to 50% of the NSC was reported in a two-stage system, with the catalyst downstream of the plasma system, whereas in a single-stage plasma−catalyst system, with the catalyst placed inside the discharge area, the NSC increased by up to 91%. Than Quoc An et al.[18] and Harling et al.[28] emphasized the higher efficiency of a one-stage-plasma−catalyst system compared with a two-stage configuration in the destruction of aromatics for environmental cleanup at room temperature. Harling et al. reported 65% destruction of toluene and 49% destruction of benzene using Ag/Al_2O_3 as the catalyst in a one-stage plasma−catalyst configuration compared with 28 and 39%, respectively, for the two-stage configuration. They attributed the enhancement in hydrocarbon destruction to the direct interaction of the radicals, electrons, and photons created by the plasma with the catalyst and molecules adsorbed on its surface. A recent example of plasma−catalyst hybrid systems with potential applications for stationary sources[29] showed promising results for low-temperature deNO_x under simulated flue gas conditions. In a combined adsorption−discharge plasma process, the adsorbed NO_x was efficiently decomposed over a H-ZSM-5 catalyst to N_2 and O_2 during the discharge stage in oxygen-deficient air and with very low space velocities. However, the addition of 2% water in the simulated flue gas caused a significant reduction in conversion. The deNO_x efficiency of the zeolite was improved by injecting 2.5% NH_3 during the discharge stage. The properties observed for combined catalyst−plasma systems show some promise for the selective NO_x reduction by hydrocarbons over Ag/Al_2O_3 catalysts, because the activation or partial oxidation of the hydrocarbons has been shown to be a controlling step in the formation of N_2 as a product.[9,27,30] Furthermore, the increased performance at low temperature of the plasma-assisted process compared with thermally activated processes may hold the solution to cold start emission control. NO_x reduction during cold start periods is still a key issue for meeting the future emission regulations, because most of the noxious emissions are released during the period when the catalysts temperature is insufficiently high to be fully active. The use of NTP for low-temperature emission control may overcome such problems.[31−33]

In the present paper, we report evidence of a nonthermal-plasma-assisted hydrocarbon selective catalytic reduction (HC-SCR) deNO_x reaction over a silver-based catalyst using He as the discharge medium. The latter was used to enable a study of whether low temperatures (25−250 °C) could be employed for the removal of NO_x using simulated diesel fuels (toluene or *n*-octane).

2. EXPERIMENTAL SECTION

2.1. Catalyst Preparation. The Ag catalyst provided by Johnson Matthey was prepared by impregnation of an γ-Al_2O_3support (LaRoche Industries, Inc.). The support material was ground and sieved to a particle size of 150−250 μm and mixed with a solution containing 0.022 M $AgNO_3$. The catalyst was then filtered, dried at room temperature for 24 h, and further dried at 100 °C for 3 h, after which the catalyst was calcined at 550 °C for 3 h.[34−36] The silver content of the catalyst was determined, using inductively coupled plasma coupled with optical emission spectroscopy (ICP-OES), to be 2 wt % Ag,[34−36] and the BET specific surface area was 170 $m^2 g^{-1}$.

2.2. Activity Tests. The experiments were designed to obtain information on the activity of the SCR catalyst when atmospheric pressure helium was used and the nonthermal plasma was in direct contact with the catalyst bed. The 2.0% Ag/Al_2O_3 catalyst sample (100 mg) was placed in the center of a fixed-bed flow reactor system, consisting of a 4 mm i.d. T-shape quartz reactor tube (Figure 1A). Typically, the catalyst

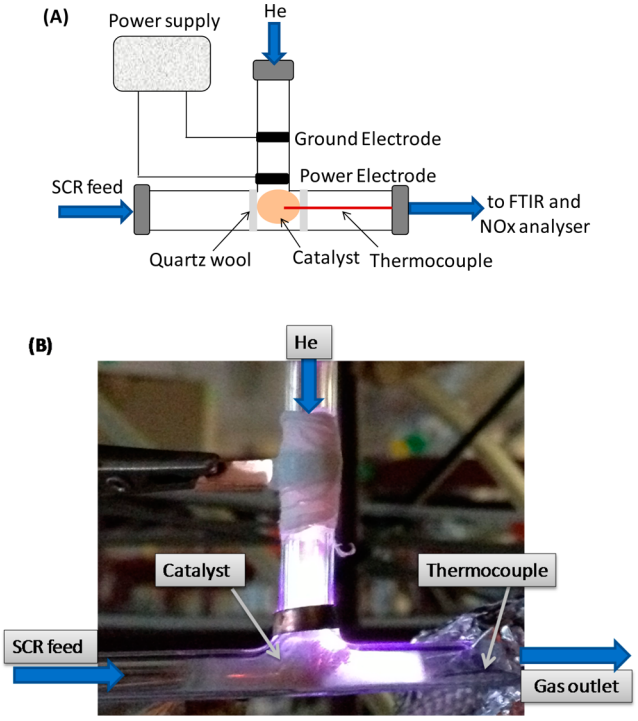

Figure 1. Schematic (A) and photograph (B) of the plasma reactor used during the HC-SCR activity test.

was held in place between plugs of quartz wool, and a K-type grounded thermocouple was placed in the center of the catalyst bed for temperature measurements in the absence of plasma. In the presence of NTP, the gas temperature was determined by analyzing the rotational N_2 plasma spectrum structure.[37−39] An Ocean Optics imaging spectrometer was used to record the spectra, which were then compared with simulated spectra of the 0−2 band of the second positive system of nitrogen at different temperatures. A least-squares procedure using Newton−Gauss algorithm was used to get the best fit between the experimental and theoretical spectral bands.[37]

The SCR gas feed stream was flowed through the horizontal tube from one side of the reactor and through the catalyst while

dx.doi.org/10.1021/cs4009286 | ACS Catal. 2014, 4, 666−673

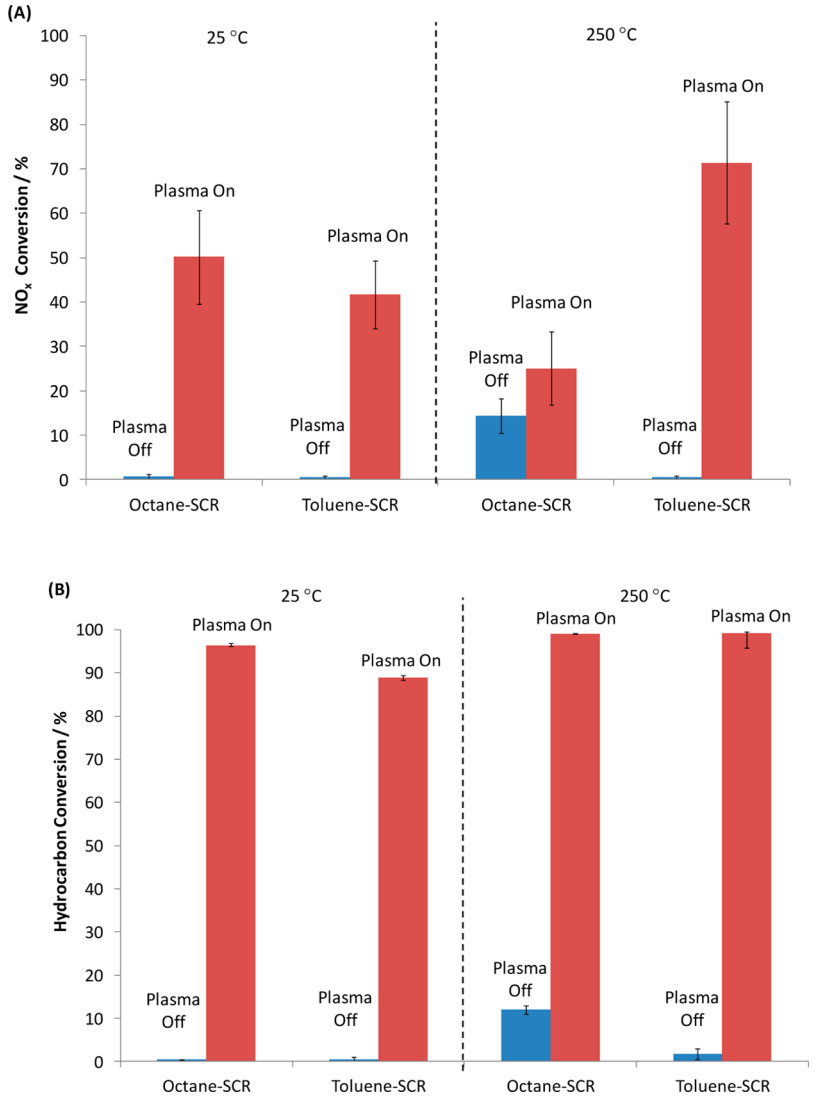

Figure 2. NO_x (A) and hydrocarbon (B) conversion during the HC-SCR of NO_x reaction over 2 wt % Ag/Al_2O_3. Feed composition: 720 ppm NO, 4340 ppm (as C1) HC, 4.3% O_2, 7.2% CO_2, 7.2% H_2O, He balance. The total flow rate and space velocity were 276 cm^3 min^{-1} and 165 600 cm^3 g^{-1} h^{-1}, respectively.

the atmospheric pressure helium for the nonthermal plasma was flowed through the vertical arm onto the catalyst, as shown in Figure 1. Helium was fed into the reactor with a flow rate of 100 cm^3 min^{-1}.

The total flow rate and space velocity of the SCR mixture were 276 cm^3 min^{-1} and 165 600 cm^3 g^{-1} h^{-1}, respectively. The gas mixture consisted of 720 ppm NO; either 540 ppm *n*-C_8H_{18} or 620 ppm toluene (corresponding to 4340 ppm as C1); 4.3% O_2; 7.2% H_2O; 7.2% CO_2; and He as the carrier gas. All the gases were supplied by BOC, and each was individually controlled by an Aera FC-7700C mass flow controller. The *n*-octane, toluene, and water vapor were introduced by passing He as a carrier gas through separate custom-made saturators. The hydrocarbon saturator was placed in an ice/water bath and the H_2O saturator temperature was controlled using a Grant GD120 thermostatic bath. All the pipework following the water saturator was heat traced to prevent condensation.

The exit of the reactor was connected in series to a Signal 4000VM series chemiluminescence detector, used to analyze the inlet and outlet NO_x concentrations, and a Bruker Tensor 27 Fourier Transform Infra-Red spectrometer (FTIR), fitted with a gas cell of volume 190 cm^3 or a Hiden Analytical HPR20 mass spectrometer (MS). The hydrocarbon conversion and gas phase CO and N_2O were monitored by FTIR, and the MS was used to monitor the formation of N_2. To quantify the dinitrogen formed, isotopically labeled ^{15}NO (m/z = 31) was used as a reactant, and the production of $^{15}N_2$ (m/z = 30) was monitored in order to avoid any interference from the fragmentation derived from the 7.2% CO_2 (m/z = 28) or any CO/CO_2 formed during the reaction. Argon was used as a tracer and internal standard. The temperature of the reaction was controlled with a calibrated hot air blower. The following equations were used to calculate the conversion of NO_x and hydrocarbon as well as the N_2, N_2O, CO_2, and CO selectivities:

$$NO_x \text{ conversion } (\%) = \frac{[NO_x]_{in} - [NO_x]_{out}}{[NO_x]_{in}} \times 100 \quad \text{(eq 1)}$$

$$\text{Hydrocarbon conversion } (\%) = \frac{[HC]_{in} - [HC]_{out}}{[HC]_{in}} \times 100 \quad \text{(eq 2)}$$

dx.doi.org/10.1021/cs4009286 | ACS Catal. 2014, 4, 666−673

Table 1. NO_x and Hydrocarbon Conversion (Conv) and Selectivity to N_2, N_2O, CO, and CO_2 during the Toluene-SCR of ^{15}NO in the Presence of the NTP Using the Blank Reactor, the Reactor in the Presence of the Thermocouple, and the Reactor in the Presence of the Thermocouple and 2% Ag/Al_2O_3 Catalyst at Ambient Temperature

	NO_x				C_7H_8			
experiment	total NO_x conv (%)	N_2 (%)	N_2O (%)	unknown (%)	HC conv (%)	CO (%)	CO_2 (%)	unknown (%)
empty reactor	4.0	trace	trace	N/A	7.5	trace	trace	N/A
blank reactor + thermocouple	24.5	75.9	2.2	21.9	71.9	13.2	73.8	13.0
2% Ag/Al_2O_3 (in the presence of the thermocouple)	42.4	96.1	1.5	2.3	89.1	10.6	90.0	N/A
	NO_x				n-C_8H_{18}			
experiment	total NO_x conv (%)	N_2 (%)	N_2O (%)	unknown (%)	HC conv (%)	CO (%)	CO_2 (%)	unknown (%)
empty reactor	11.5	trace	trace	N/A	4.5	trace	N/A	N/A
blank reactor + thermocouple	34.8	75.9	23.8	0.3	79.2	9.2	90.1	0.7
2% Ag/Al_2O_3 (in the presence of the thermocouple)	51.7	77.9	21.5	0.6	98.8	13.5	86.1	0.4

$$N_2 \text{ selectivity } (\%) = \frac{2[N_2]}{[NO_x]_{in} - [NO_x]_{out}} \times 100 \quad \text{(eq 3)}$$

$$N_2O \text{ selectivity } (\%) = \frac{2[N_2O]}{[NO_x]_{in} - [NO_x]_{out}} \times 100 \quad \text{(eq 4)}$$

$$CO_2 \text{ selectivity } (\%) = \frac{[CO_2]}{x\{[C_xH_y]_{in} - [C_xH_y]_{out}\}} \times 100 \quad \text{(eq 5)}$$

$$CO \text{ selectivity } (\%) = \frac{[CO]}{x\{[C_xH_y]_{in} - [C_xH_y]_{out}\}} \times 100 \quad \text{(eq 6)}$$

A dielectric barrier discharge was created in the vertical tube by applying a voltage to the lower of the two external circular copper electrodes, based on the system described by Teschke et al.,[40] while the upper electrode was grounded. In addition, the thermocouple placed within the reactor acted as an internal grounded electrode. A high voltage probe (Tektronix, P6015) and a calibrated Rogowski coil (Pearson) connected to a digital oscilloscope (LeCroy WavePro 7300A) were used to measure the variable, time-dependent applied voltage and current. The powered electrode was driven at peak voltages from 6 to 7 kV and modulated from 16 to 23 kHz. Time-resolved voltage and current measurements showed that the power into the plasma was between 1 and 2 W.

3. RESULTS AND DISCUSSION

3.1. Activity Tests. Figure 2 shows the deNO$_x$ performance of the Ag catalyst at 25 and 250 °C using *n*-octane and toluene in the absence and presence of the NTP. Figure 2A clearly shows that, at ambient temperature and in the presence of the NTP, NO_x conversions of ∼52% in the case of *n*-octane and ∼42% in the case of toluene were obtained with N_2 selectivities of ∼78 and 96%, respectively. For *n*-octane-SCR, the N_2O selectivity was 21.5%, with 0.6% of unidentified N-containing compounds present. For toluene-SCR, the N_2O selectivity was ∼2%, and 2% of unidentified N-containing compounds were also observed. NH_3 was not detected under any of the conditions explored. No activity was observed when the plasma was not applied.

Further reduction of NO_x in the presence of toluene was obtained by increasing the temperature of the reaction to 250 °C. In the presence of the NTP (Figure 2), the conversion of NO_x reached ∼70%, with 99% selectivity to N_2 and ∼1% to N_2O. Again, no conversion was observed in the absence of the NTP. A different trend was observed in the case of the *n*-octane-SCR, where the increase in temperature led to a decrease of the NO_x conversion to ∼25%, with more than 75% selectivity toward N_2. This effect will be discussed in section 3.2. A small increase in NO_x conversion was noted at 250 °C in the absence of NTP.

Figure 2B shows that when the reaction was carried out at ambient temperature, the presence of the NTP led to >98% conversion of the *n*-octane and ∼89% conversion of the toluene, compared with <5% when the NTP was not applied. Increasing the reaction temperature to 250 °C resulted in full consumption of the hydrocarbons.

Of major importance is the assessment of the synergetic effect of the NTP + catalyst in the enhancement of the SCR activity at low temperatures. A comparison of the conversions and selectivities for reactions performed using the NTP in the empty reactor, the empty reactor in the presence of the thermocouple and in the presence of the catalyst within the NTP together with the thermocouple is reported in Table 1. The presence of the catalyst in the discharge area had a major effect on the conversion of the hydrocarbons and NO_x. For the toluene-SCR, in the presence of the NTP, the total NO_x conversion was found to be <5% in the empty reactor with an increase to ∼25% upon the introduction of the thermocouple into the reactor. In the presence of the thermocouple and the 2% Ag/Al_2O_3 catalyst within the plasma discharge area, the total NO_x conversion with toluene in the feed was ∼42%. A similar trend was observed for the toluene conversion with ∼8% found using the empty reactor with the NTP compared with ∼72% in the presence of the thermocouple and ∼89% in the presence of the catalyst and thermocouple. A 20% decrease in N_2 formation was observed in the absence of the catalyst with the thermocouple acting as a second ground electrode, whereas insignificant quantities of N_2 were formed when the thermocouple was removed. The selectivity toward CO_2 was also improved in the presence of the catalyst and thermocouple compared with the empty reactor in the presence of the thermocouple. In the former case, 90% selectivity to CO_2 was observed compared with ∼74% in the latter arrangement. Importantly, the change in the CO_2 selectivity is not due to a significant change in the CO selectivity which only decreases from ∼13 to 11% on addition of the catalyst. The presence of the catalyst in the NTP eliminates the formation of other C-containing byproducts, reported as "unknown products" in

dx.doi.org/10.1021/cs4009286 | ACS Catal. 2014, 4, 666−673

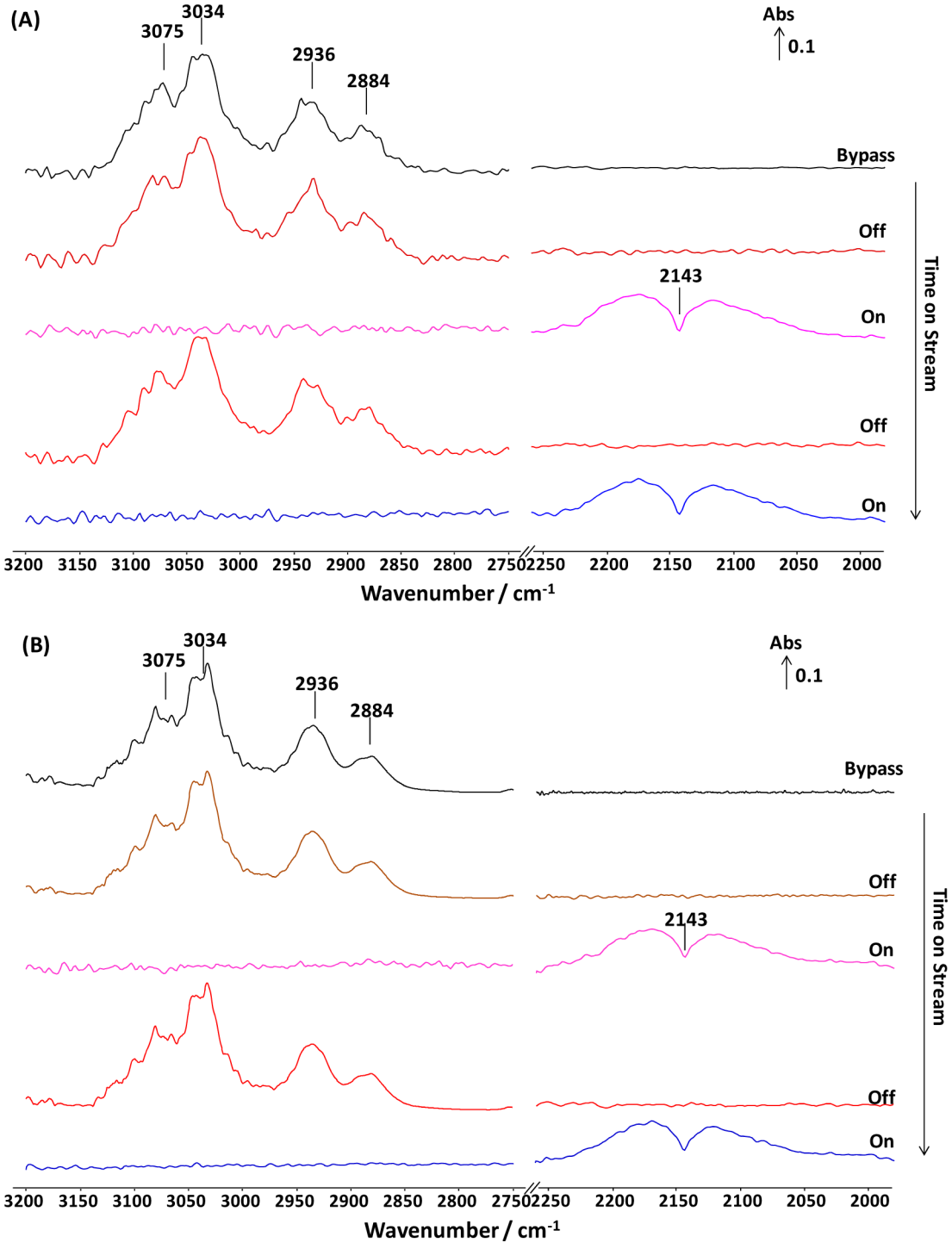

Figure 3. FTIR spectra of gas phase species recorded during switching 7 kV, 19 kHz plasma on and off under toluene-SCR of NO_x reaction conditions over 2% Ag/Al_2O_3 catalyst at (A) 250 °C and (B) 25 °C. Feed conditions: 720 ppm NO, 4.3% O_2, 4340 ppm (as C_1) toluene, 7.2% CO_2, 7.2% H_2O, He Balance. The total flow rate and space velocity were 276 cm^3 min^{-1} and 165 600 cm^3 g^{-1} h^{-1}, respectively.

Table 1. In the absence of the catalyst, these represent 13% of the carbon balance. Note that under the latter conditions, the reactor and quartz wool became discolored.

Similarly, very low conversions were observed for the activity test on the empty reactor, in the absence of both catalyst and thermocouple for the plasma-assisted *n*-octane-SCR. In general, higher NO_x and hydrocarbon conversion were observed for the plasma-assisted *n*-octane-SCR, and the trends were similar to those observed for toluene (i.e., an increase in conversions when the thermocouple was connected to the system and further improvement in the SCR activity when the catalyst was positioned in the discharge area). Importantly, despite the increase in NO_x conversion from ∼35% in the empty reactor with the thermocouple to ∼52% in the presence of the catalyst and thermocouple, no significant changes were observed in the formation of $^{15}N_2$ (∼76% compared with ∼78%, respectively). This is a significant difference compared with the toluene-SCR

dx.doi.org/10.1021/cs4009286 | *ACS Catal.* 2014, 4, 666−673

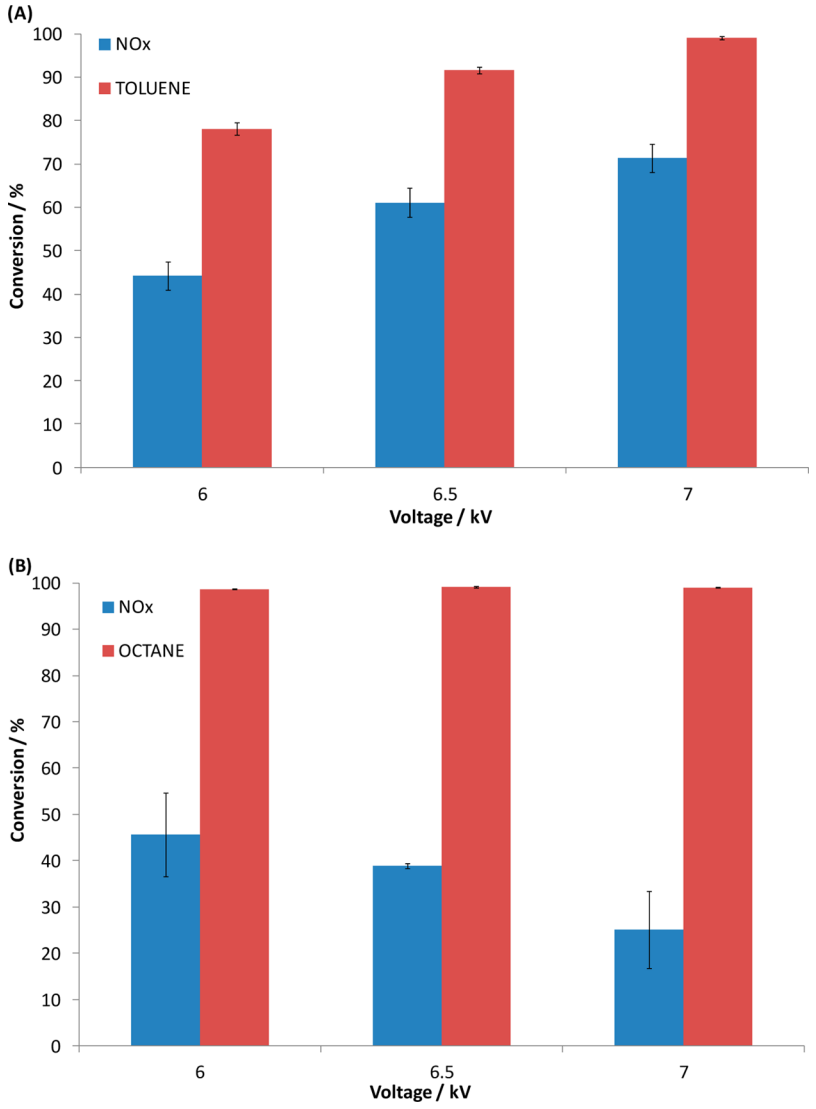

Figure 4. Effect of applied voltage on the NO_x conversion at 19 kHz during the SCR reaction over 2 wt % Ag/Al_2O_3 with toluene (A) and *n*-octane (B) at 250 °C. Feed conditions: 720 ppm NO, 4.3% O_2, 4340 ppm (as C_1) HC, 7.2% CO_2, 7.2% H_2O, He Balance. The total flow rate and space velocity was 276 cm^3 min^{-1} and 165 600 cm^3 g^{-1} h^{-1}, respectively.

reaction, which showed ∼96% selectivity to N_2 in the presence of the catalyst and thermocouple.

The presence of water is known to be important for the thermally activated HC-SCR reaction. Recent results showed that in the absence of water only 20% conversion of NO_x was observed in comparison to 60% following the addition of 7.2% of water at 400 °C.[41] Figure S1 shows the effect of the addition of water into the HC-SCR feed during the NTP-activated reaction. In comparison with the SCR with H_2O, the SCR without H_2O showed a decrease in the NO_x and toluene conversion from ∼40 to 18% and from ∼90 to 80%, respectively. No significant changes in selectivity were observed.

Further experiments were performed to investigate the behavior of the gas species when switching the plasma on and off during the toluene-SCR reaction at 250 °C. FTIR spectra of the gas phase outlet as a function of switching the plasma on and off are reported in Figure 3A. When compared with the IR spectra recorded when bypassing the reactor and when the plasma was off, significant differences could be observed in the presence of the plasma. With an applied electrode voltage of 7 kV, it was found that the IR bands between 3100 and 2800 cm^{-1}, assigned to the vibrational C−H stretching of gas phase toluene, disappeared. This indicated that toluene had been activated for NO_x reduction and at least partially converted to form gas phase CO_2 (not shown) and CO (see Figure 3), as shown by the bands at 2143 cm^{-1}.[42,43] No significant lag was observed between the gas phase spectra and presence or absence of the plasma indicating that the species formed are short-lived and only affect the activity when the plasma is applied.

Similar effects on the hydrocarbon oxidation during plasma on−off switches were observed when the test was performed at room temperature (Figure 3B). Importantly, during these switches, the temperature of the gas was determined from the rotational structure of the N_2 second positive system emission. The measurements were done at a distance between the reactor and the optical probe of ∼12 mm. Figure S2 shows the best fit of simulated spectrum with the experimental data of the nitrogen emission line (377−381 nm), which corresponds to a rotational gas temperature of 93 °C for the *n*-octane-SCR reaction and 91 °C for the toluene-SCR reaction. Furthermore,

dx.doi.org/10.1021/cs4009286 | ACS Catal. 2014, 4, 666−673

the response of the thermocouple probe after switching off the plasma also showed a temperature of ~120 °C, indicating that thermal activation of the catalyst is not likely to be the cause of the enhanced activity observed.

Further studies were performed using different reactor configurations to assess their impact on the plasma's reactor performance. It was found that placing the plasma upstream of the catalyst or above but not passing through the catalyst bed had little effect on the NO_x conversion. The schematics of all the reactor configurations tested are presented in the Supporting Information (Figure S3).

3.2. Effect of the Voltage and the Frequency on the Plasma Reactor Efficiency. Figure 4 shows the effect of the applied voltage on plasma-assisted SCR of NO_x and hydrocarbon conversion at 250 °C. An increase in voltage from 6 to 7 kV resulted in an increase in the toluene conversion from ~78 to 99% together with the NO_x conversion increasing from 44 to 71% (Figure 4A). A different trend was observed when using *n*-octane as the reductant. Figure 4B shows that the NO_x conversion decreased from ~45 to 25% on increasing the voltage from 6 to 7 kV, although the *n*-octane was fully converted.

There is a general agreement that the activation of the hydrocarbon is a key step in the mechanism of HC-SCR of NO_x. It has been discussed and accepted by many researchers that the activation of both NO_x and hydrocarbons leads to the formation of surface NCO species, which is thought to be a key intermediate and involved in the final step of the SCR reaction over Ag/Al_2O_3 catalysts to form N_2.[33−36,42−45] It was reported that aromatics (toluene in this case) are inactive at temperatures below 400 °C.[5,46,47] This would indicate that the activation and partial oxidation of toluene requires more energy and subsequently a higher temperature than *n*-octane. The SCR activity with toluene shown in Figure 4A was enhanced at low temperatures with increasing voltage. This is probably due to increased plasma energy applied at the higher voltages, which promoted the activation and partial oxidation of toluene and subsequently led to increased $deNO_x$ activity. In contrast, as *n*-octane is easier to activate, an increase in the energy either by increasing the voltage or the temperature of the reaction (as shown in Figure 2) led to overoxidation of the hydrocarbon favoring total combustion rather than reaction with NO_x. This is similar to the effect observed in the thermally activated HC-SCR $deNO_x$ reactions, where increases in temperature initially lead to increased NO_x conversion, where partial oxidation of the HC occurs. At sufficiently high temperatures, total combustion of the hydrocarbon is dominant, and the NO_x conversion decreases.

The driving frequency also had a significant effect on the HC-SCR of NO_x. Figure S4A shows the NO_x conversion obtained during the *n*-octane-SCR reaction performed at 250 °C as a function of the driving current frequency at 6 kV. The NO_x conversion was found to decrease from 63% at ~16 kHz to 45% at ~20 kHz. This behavior mirrors the trends obtained with increasing voltages. An increase in driving frequency increases the plasma energy density and, therefore, if the energy provided exceeds that required, this will lead to an enhancement of the selectivity toward total combustion and finally a reduced SCR performance. Furthermore, by varying the driving frequency not only is the NO_x conversion affected but also the N_2O selectivity, as shown in Figure S4B. This is consistent with the results from thermal activation where the formation of N_2O depends both on the NO_x conversion and on the temperature,[1] following a volcano curve. Therefore, it was possible to maximize the selectivity toward N_2 compared with N_2O by controlling the reaction temperature as well as the driving frequency, leading to <15% N_2O formation at 250 °C using a voltage of 6 kV and a frequency of 16.3 kHz. However, further fine-tuning of the voltage/frequency and the duration of the pulse is required in order to enhance the SCR activity for the Ag-based catalyst at low temperature.

4. CONCLUSIONS

An atmospheric pressure nonthermal plasma catalytic reactor was developed. When combined with an Ag/Al_2O_3catalyst and applied to HC-SCR of NO_x, a strong enhancement was observed when compared with conventional thermal activation. In the presence of the plasma, high conversions of both NO_x and hydrocarbons were obtained at temperature ≤250 °C, where the silver-based catalyst is normally inactive. Importantly, significant activity was obtained at 25 °C. These results provide a promising base for future development of vehicle exhaust treatment during cold start, which remains a serious problem in terms of pollutants emissions.

■ ASSOCIATED CONTENT

Ⓢ Supporting Information

Contains the effect of water on the toluene-SCR reaction, the experimental and simulated emission spectra during the HC-SCR reactions, the schematics of the reactor configurations tested and effect of applied current frequency on the HC-SCR reactions. This material is available free of charge via the Internet at http://pubs.acs.org.

■ AUTHOR INFORMATION

Corresponding Authors

*E-mail: c.hardacre@qub.ac.uk.
*E-mail: b.graham@qub.ac.uk.

Notes

The authors declare no competing financial interest.

■ ACKNOWLEDGMENTS

The authors would like to thank EPSRC for financial support through the CASTech project (EP/G02152X/1), and W.A. acknowledges the support of the Iraqi Ministry of Higher Education and Scientific Research.

■ REFERENCES

(1) Burch, R.; Breen, J. P.; Meunier, F. C. *Appl. Catal., B* **2002**, *39*, 283−303.
(2) Iglesias-Juez, A.; Hungría, A. B.; Martínez-Arias, A.; Fuerte, A.; Fernándezcía, M.; Anderson, J. A.; Conesa, J. C.; Soria, J. *J. Catal.* **2003**, *217*, 310−323.
(3) Lindfors, L.-E.; Eränen, K.; Klingstedt, F.; Murzin, D. Y. *Top. Catal.* **2004**, *28*, 185−189.
(4) He, H.; Yu, Y. *Catal. Today* **2005**, *100*, 37−47.
(5) Shimizu, K.; Satsuma, A. *Phys. Chem. Chem. Phys.* **2006**, *8*, 2677−2695.
(6) Takagi, K.; Kobayashi, T.; Ohkita, H.; Mizushima, T.; Kakuta, N.; Abe, A.; Yoshida, K. *Catal. Today* **1998**, *45*, 123−127.
(7) Sultana, A.; Haneda, M.; Fujitani, T.; Hamada, H. *Catal. Lett.* **2007**, *114*, 96−102.
(8) Li, J.; Zhu, Y.; Ke, R.; Hao, J. *Appl. Catal., B* **2008**, *80*, 202−213.
(9) Li, J.; Ke, R.; Li, W.; Hao, J. *Catal. Today* **2007**, *126*, 272−278.
(10) Kannisto, H.; Ingelsten, H. H.; Skoglundh, M. *J. Mol. Catal. A: Chem.* **2009**, *302*, 86−96.

(11) Martínez-Arias, A.; Fernández-García, M.; Iglesias-Juez, A.; Anderson, J. A.; Conesa, J. C.; Soria, J. *Appl. Catal., B* **2000**, *28*, 29−41.
(12) Shimizu, K.; Satsuma, A.; Hattori, T. *Appl. Catal., B* **2000**, *25*, 239−247.
(13) Shimizu, K.; Shibata, J.; Yoshida, H.; Satsuma, A.; Hattori, T. *Appl. Catal., B* **2001**, *30*, 151−162.
(14) Mizuni, A. *Catal. Today* **2013**, *211*, 2−8.
(15) Hessel, V.; Anastasopoulou, A.; Wang, Q.; Kolb, G.; Lang, J. *Catal. Today* **2013**, *211*, 9−28.
(16) Oda, T. *J. Electrost.* **2003**, *57*, 293−311.
(17) Durme, J. V.; Dewulf, J.; Leys, C.; Langenhove, H. V. *Appl. Catal., B* **2008**, *78*, 324−333.
(18) Than Quoc An, H.; Pam Huu, T.; Le Van, T.; Cormier, J. M.; Khacel, A. *Catal. Today* **2011**, *176*, 474−477.
(19) Tang, X.; Feng, F.; Ye, L.; Zhang, X.; Huang, Y.; Liu, Z. *Catal. Today* **2013**, *211*, 39−43.
(20) Shi, C.; Zhang, Z.; Crocker, M.; Xu, L.; Wang, C.; Au, C.; Zhu, A. *Catal. Today* **2013**, *211*, 96−103.
(21) Zhou, T.; Jang, K.; Lang, B. W. L. *Catal. Today* **2013**, *211*, 147−155.
(22) Lee, D. H.; Lee, J.-O.; Kim, K.-T.; Song, Y.-H.; Kim, E.; Han, H.-K. *Int. J. Hydrogen Energy* **2011**, *36*, 11718−11726.
(23) Lee, D. H.; Lee, J.-O.; Kim, K.-T.; Song, Y.-H.; Kim, E.; Han, H.-K. *Int. J. Hydrogen Energy* **2012**, *37*, 3225−3233.
(24) Wang, H.; Li, X.; Chen, M.; Zheng, X. *Catal. Today* **2013**, *211*, 66−71.
(25) Matsumoto, T.; Wang, D.; Namihira, T.; Akiyama, H. *InTech* **2012**, 215−234.
(26) Rappé, K. G.; Hoard, J. W.; Aardahl, C. L.; Park, P. W.; Peden, C. H. F.; Tran, D. N. *Catal. Today* **2004**, *89*, 143−150.
(27) Cho, B. K.; Lee, J.-H.; Crellin, C. C.; Olson, K. L.; Hilden, D. L.; Kim, M. K.; Kim, P. S.; Heo, I.; Oh, S. H.; Nam, I.-S. *Catal. Today* **2012**, *191*, 20−29.
(28) Harling, A. M.; Demidyuk, V.; Fischer, S. J.; Whitehead, J. C. *Appl. Catal., B* **2008**, *82*, 180−189.
(29) Wang, H. *Chem. Commun.* **2013**, *49*, 9353−9355.
(30) Magureanu, M.; Piroi, D.; Mandache, N. B.; Pârvulescu, V. I.; Pârvulescu, V.; Cojocaru, B.; Cadigan, C.; Richards, R.; Daly, H.; Hardacre, C. *Appl. Catal., B* **2011**, *104*, 84−90.
(31) Okubo, M.; Tanioka, A.; Kuroki, T.; Yamamoto, T. *IEEE Trans. Ind. Appl.* **2002**, *38*, 1196−1203.
(32) Kim, H. H.; Ogata, A.; Futamura, S. *Appl. Catal., B* **2008**, *79*, 256−267.
(33) Yu, Q. Q.; Wang, H.; Liu, T.; Xiao, L. P.; Jiang, X. Y.; Zheng, X. M. *Environ. Sci. Technol.* **2012**, *46*, 2337−2344.
(34) Chansai, S.; Burch, R.; Hardacre, C.; Breen, J.; Meunier, F. *J. Catal.* **2010**, *276*, 49−55.
(35) Chansai, S.; Burch, R.; Hardacre, C.; Breen, J.; Meunier, F. *J. Catal.* **2011**, *281*, 98−105.
(36) Breen, J. P.; Burch, R.; Hardacre, C.; Hill, C. J.; Rioche, C. *J. Catal.* **2007**, *246*, 1−9.
(37) Twomey, B.; Nindrayog, A.; Niemi, K.; Graham, W. G.; Dowling, D. P. *Plasma Chem. Plasma Process.* **2011**, *31*, 139−156.
(38) Lu, X.; Xiong, Q.; Xiong, Z.; Hu, J.; Zhou, F.; Gong, W.; Xian, Y.; Zou, C.; Tang, Z.; Jiang, Z.; Pan, Y. *J. Appl. Phys.* **2009**, *105*, 043304.
(39) Faure, G.; Shkolnik, S. M. *J. Phys. D: Appl. Phys.* **1998**, *31*, 1212−1218.
(40) Teschke, M.; Kedzierski, J.; Finan-Dinu, E. G.; Korzec, D.; Engrmann, J. *IEEE Trans. Plasma Sci.* **2005**, *33*, 310−311.
(41) Ralphs, K.; D'Agostino, C.; Burch, R.; Chansai, S.; Gladden, L. F.; Hardacre, C.; James, S. L.; Mitchell, J.; Taylor, S. F. R. *Catal. Sci. Technol.* **2014**, *4*, 531−539.
(42) Meunier, F. C.; Breen, J. P.; Zuzaniuk, V.; Olsson, M.; Ross, J. R. H. *J. Catal.* **1999**, *187*, 493−505.
(43) Bion, N.; Saussey, J.; Haneda, M.; Daturi, M. *J. Catal.* **2003**, *217*, 47−58.
(44) Tamm, S.; Ingelsten, H. H.; Palmqvist, A. E. C. *J. Catal.* **2008**, *255*, 304−312.
(45) Eränen, K.; Klingstedt, F.; Arve, K.; Lindfors, L.-E.; Murzin, D. Y. *J. Catal.* **2004**, *227*, 328−343.
(46) Demidyuk, V.; Hardacre, C.; Burch, R.; Mhadeshwar, A.; Norton, D.; Hancu, D. *Catal. Today* **2011**, *164*, 515−519.
(47) Kim, M. K.; Kim, P. S.; Baik, J. H.; Nam, I.-S.; Cho, B. K.; Oh, S. H. *Appl. Catal., B* **2011**, *105*, 1−14.